



Removal of natural organic matter (NOM) by ion exchange from surface water for drinking water production: a pilot-scale study

Wim T.M. Audenaert, Lisa Van Beneden, Stijn W.H. Van Hulle*

LIWET, Departement of Industrial Biological Sciences, Ghent University, Campus Kortrijk, Graaf Karel de Goedelaan 5, B-8500 Kortrijk, Belgium, Tel. +32 56241251; Fax: +32 56241224; emails: Wim.Audenaert@UGent.be (W.T.M. Audenaert), Lisa.VanBeneden@UGent.be (L. Van Beneden), Stijn.VanHulle@UGent.be (S.W.H. Van Hulle)

Received 26 March 2015; Accepted 6 June 2015

ABSTRACT

Natural organic matter (NOM) in drinking water causes esthetic concerns such as odor, taste, and color and is responsible for the disinfection byproducts formation during drinking water production. The goal of this study was to determine the efficiency of macroporous polyacrylic ion exchange resins for the removal of NOM as a function of empty bed contact time (EBCT), bed expansion, and regeneration procedure. Two resins were examined: the coarse Purolite®PPA860S and the fine Purofine®PFA860 resin. The tests showed that both resins are suitable for NOM removal. The reduction in particle size (beads of the fine resin were 18% smaller than those of the coarse one) of the fine resin had little effect on NOM removal, although the exchange capacity of the fine resin after regeneration was 12% higher than that of the coarse resin after multiple regenerations. The influence of SO_4^{2-} (due to the re-use of the regenerating solution) was examined on the basis of a regeneration solution with only SO_4^{2-} . The test results showed no reduction in NOM removal during prolonged operation. Finally, it was concluded that the EBCT can be significantly reduced as increasing the flow velocity from 15 to 20 m/h did not result in a significant reduction in NOM removal efficiency.

Keywords: Ion exchange; Natural organic matter; Drinking water production; Humic acids; HPSEC; Spectral changes

1. Introduction

Each type of water naturally contains an amount of natural organic matter (NOM), at a concentration of about 0.2–10 mg/l [1]. NOM can be either autochthonous from natural aquatic processes, or coming from external sources such as land run-off. Autochthonous NOM typically includes metabolites and decomposition products of algae, bacteria, and other microorganisms. Organic material from external sources

originates from leaching of soil and degradation of external organic material. The complexity of NOM is large, knowing that many factors can influence and characterize NOM such as the soil composition, weather conditions, climate, vegetation, and animal and human activities [2]. NOM can be further divided into the humic (hydrophobic)—and non-humic (hydrophilic) fraction [3]. The humic components consist mainly of fulvic and humic acids and represent about 50–65% of the dissolved organic material in surface waters [4].

*Corresponding author.

NOM by itself is harmless to humans. However, the presence of NOM during drinking water production results in odor, taste, and color problems and leads to formation of harmful byproducts and regrowth of micro-organisms in the distribution system [5]. NOM may form bonds with heavy metals such as Cu, Pb, and Hg, or heavy organic compounds such as PCBs (polychlorinated biphenyls), DDT (insecticide $C_{14}H_9Cl_5$), and PAHs (polycyclic aromatic hydrocarbons) [5]. NOM in drinking water also affects the biological stability. Biodegradable NOM stimulates the growth of micro-organisms. Insufficient removal of NOM may give rise to decreased biological stability of the water and regrowth of micro-organisms [6].

Certain NOM fractions can have a strong influence on the water treatment processes. Activated carbon filtration is adversely affected by preferential adsorption of NOM and blockage of the macropores. During the coagulation/flocculation process, NOM forms complexes with iron and aluminum salts, leading to higher required doses of these coagulants and greater sludge production. In the presence of NOM during oxidation processes, potential formation of disinfection byproducts (DBPs) occurs [5]. During ozonation, unwanted assimilable organic carbon may be formed [5]. Upon addition of chlorine, trihalomethanes (THM) and halogenated acetic acids can occur [4].

The removal of NOM is therefore an important step during drinking water production. One of the techniques that can be used is ion exchange. Strongly basic anion resins are used for this purpose. These resins exchange their chlorides with negatively charged NOM. Besides NOM, also inorganic ions (such as SO_4^{2-} , CO_3^{2-}) are removed [7]. The ion exchange process is reversible, which enables the reuse of the resins after regeneration. During regeneration, the resin is converted back into the chloride form, and NOM is removed with the regeneration solution. This regeneration solution is usually NaCl solution, because of its low cost and relatively inert behavior. Also, other salts, such as $NaHCO_3$ can be applied [8].

The optimization of NOM removal by means of ion exchange has been a subject of intense research for the last 10 years. Low NOM levels are required in order to use less chemicals in the downstream processing steps such coagulation/flocculation. For a case study, the largest water production center (WPC) of the Flemish drinking water company “De Watergroep” in Kluizen [9,10] is taken. The current treatment line (constructed in 2007) removes NOM using coagulation/flocculation with polyaluminum chloride (PAC) and subsequent flotation. By 2018, an ion exchange system placed before the coagulation/flocculation unit will support the possible capacity

increase to 45,000 m³/d. In preparation for this, it is necessary to optimize the ion exchange process for the removal of NOM.

There are several aspects to play a role in such optimization such as for example the type of resin. Macroporous resins have a higher degree of cross-linking, making them less prone to swelling. In addition, they have larger pores than gel resins, which promote the removal of the larger NOM molecules. Bolto et al. [11], for example, compared the incorporation of NOM with a larger molecular weight (MW) by a macroporous resin with a gel resin. Because of the more open structure of the macroporous resin, the NOM was absorbed much faster by the macroporous resin. The MW of the NOM also has a strong impact on the removal efficiency. Phetrak et al. [12] investigated raw water that contained NOM with MW of 700–4,000 Da. Especially, NOM greater than 1,000 Da was removed by the resin that could achieve this removal in shorter time because of the macroporous structure and small particle size. Smaller NOM (<1,000 Da) remains in the water after treatment [12]. NOM with a larger MW can further prevent ion exchange by clogging the pores of the resin surface. For example, NOM with MW greater than 5,000 Da was poorly removed by the macroporous resin MIEX[®] [13]. A smaller particle size further results in a larger specific surface area and in that way a larger exchange surface. This results in a higher exchange capacity or in other words in a faster removal of NOM [14,15]. As such, resins with smaller particle sizes can remove NOM fractions with low to medium MW efficiently, but then again prove less effective for removing NOM with large MW. Resins with smaller particle sizes have a less open structure, hence reducing the penetration of larger NOM fractions. In this way, there is less NOM present in the resin particle itself compared to larger particles. Together with the shorter diffusion paths of small resin particle, this results in a better resistance to fouling, and a better exchange of ions [16]. Nguyen et al. [10] finally illustrate the impact of the empty bed contact time (EBCT) on the dissolved organic carbon (DOC) removal with the MIEX[®] resin. When increasing the flow rate (and therefore lowering the EBCT), there is a decrease of the NOM removal. Hongve et al. [17] concluded from the experiments with a strong anionic resin that NOM with a low MW and high charge density is easily removed. Larger molecules penetrate less efficiently inside the resin and are thus less removed by the resin. A larger EBCT is thus required in order to remove these larger molecules. Finally, there is the bed expansion. Resins expand more if they have a smaller particle size and as the temperature is low [18]. With increasing operation time, the density and

particle size of the resin increase, resulting in a decrease of the bed height (and thus the bed expansion). The increased density and particle sizes are the result of the increase in the amount of NOM on the particle [18].

It is thus clear that several factors play a role in the optimization of the ion exchange process for the removal of NOM. The characterization of NOM was done on the basis of various parameters: DOC, UV-absorption coefficient at 254 nm (UVA_{254}), specific ultraviolet absorbance (SUVA ($=UVA_{254}/DOC$)), and size exclusion measurements. This study compares the efficiency of two resins with different particle sizes for the removal of NOM as a function of EBCT, bed expansion, and regeneration during pilot-scale operation. The decrease in the capacity of the resins overtime was taken into account. Also the impact of ion exchange on NOM characteristics was studied based on multiple measurements.

2. Materials and methods

2.1. Applied resins

The tested resins were the coarse Purolite®PPA860S resin and the fine Purofine®PF860 resin, which will be referred to as the coarse resin and the fine resin, respectively. Both resins are type-1 polyacrylic anion resins. These anion resins contain a quaternary ammonium group in which Cl^- ions are bound. The properties are listed in Table 1. These types were chosen based on preliminary research conducted at the WPC [30] and due to their relatively low cost.

2.2. Experimental pilot set-up

The influence of resin type and bead size, EBCT, bed expansion, and regeneration on the efficiency of the process was investigated by characterizing the effluent NOM, measuring the bed height and conductivity measurements.

The experiments took place in an open cylindrical column (diameter: 10 cm) (described previously by Verdickt et al. [19]) at a maximum flow rate of 200 l/h (25.5 m/h). The column contained 2 l resin. The column is fed at the bottom through a dispenser, while the effluent left the column at the top by means of an overflow system. Controlled valves make it possible to incorporate automatic sampling.

The average composition of the influent during tests with fine and coarse resin is presented in Table 2. A nominal flow rate of 120 l/h (15.3 m/h; 60 s EBCT) was applied for all experiments, except for an experiment during which the effect of flow velocity was tested.

Batch regeneration of the total resin content was performed every 1,500 bed volumes (BVs, 3,000 l) which implied that operation of the column was stopped during regeneration. The total amount of resin is regenerated, while in the envisioned continuous full-scale installation this is only 3–4%. For regeneration, the column was drained after which 1 BV (2 l) of regeneration brine was added on top of the column and collected at the bottom. After having rinsed the resin with 4 l of water, operation was resumed. A brine solution (pH 6.2 and DOC concentration of 500 mg C/l) of 1 eq/l Cl^- and 0.3 eq/l SO_4^{2-} was used for all experiments. Also the effect of regeneration with a pure SO_4^{2-} solution (1.3 eq/l) was investigated, as during full-scale application the regeneration solution is reused and as such SO_4^{2-} can be expected to accumulate in the brine.

The experimental period between two regenerations is called a run. On average, runs lasted 24 h. A (full) test cycle consists of several consecutive runs and starts with the introduction of fresh resin. First three stabilizing runs are carried out without measurements. In the first runs, the difference in NOM removal between runs is large, because of the use of fresh resin. After three stabilizing runs, the measurements of different runs become similar and can be considered reliable. In a run, nine samples are taken at different bed volumes (0, 20, 50, 100, 200, 300, 600, 900, 1,200, and 1,500 BV) using automatically controlled valves.

2.3. Overview of the performed measurements

2.3.1. Direct and derived measurements during column experiments

The HPSEC analysis was performed with an Agilent HPLC (Agilent 1100 series) with fluorescence and diode-array detector (DAD). DAD measures a spectrum at 200–400 nm with a resolution of 1 nm. A Shodex Protein KW-802.5 column with pre-column was used for the separation. The mobile phase was 10 times diluted in 0.02-M phosphate buffer (K_2HPO_4 and K_2PO_4) with a pH of 6.8. In order to avoid solvent peaks, a buffer solution with the same concentration as the mobile phase was added to each sample [20].

The UV-Vis spectrophotometer (Shimadzu UV-1601) measured a broad spectrum (200–800 nm) with a resolution of 0.5 nm from the different samples. The Hach single-beam UV/Vis spectrometer DR5000 was used to measure onsite the absorbance at 254 nm (UVA_{254}).

From the UV-Vis spectra, Differential absorbance spectra (DAS) were calculated. DAS is defined as the

difference between the influent absorbance spectrum and the spectrum after several bed volumes. If the DAS is divided by the differential absorbance at the wavelength at which the DAS reaches its maximum, then a normalized DAS is obtained.

Furthermore, from the UV–Vis spectra and the HPSEC chromatograms the absorbance slope index (ASI) is determined. The ASI is calculated on the basis of the following Eq. (1) [20,21].

$$\text{ASI} = 0.56 \left(\frac{\text{UVA}_{254} - \text{UVA}_{272}}{\text{UVA}_{220} - \text{UVA}_{230}} \right) \quad (1)$$

The DOC was measured according to the ISO 8245:1999 procedure. The specific UVA_{254} (SUVA) was calculated by dividing the average UVA_{254} values by the average DOC values. High SUVA values (>4) indicate hydrophobic, aromatic compounds while low SUVA values (<3) on the other hand indicate more hydrophilic components [3].

The conductivity was measured with a WTW (Xylem brand) conductivity meter. The ions Cl^- and SO_4^{2-} were measured during the column test by ion chromatography according to the ISO 10304-1:2007 procedure. For the resin characterization, other methods were used as indicated below.

2.3.2. Resin characterization

The bed expansion is easily measured by a ruler as the column is transparent. For the determination of the exchange capacity of both fresh and used resin, the quality control test method for a strong anion resins from the manufacturer (Purolite) was used. The capacity determination begins with the reaction of 25-ml resin (resin density of 1.08 g/ml) for 60 min with 1% NaNO_3 . A burette with a filter at the bottom is used for this in order to pass 1 l NaNO_3 -solution at a constant speed through 25 ml of resin. This results in 1 l effluent.

An initial titration with 0.1 M HCl in 100 ml effluent, to which 3 drops of bromocresol green indicator (pH transition range 3.8–5.4) is added, is carried out for the determination of the concentration of CO_3^{2-} (eq/l).

For the determination of the Cl^- concentration (eq/l), 100-ml effluent is acidified and then neutralized with NaCO_3 . For the titration with 0.1-M AgNO_3 , a K_2CrO_4 indicator is used. Also a blank sample is titrated to correct for possible measurement errors.

The SulfaVer[®] 4 method using a colorimeter (Hach DR890) was used for the measurement of the concentration of SO_4^{2-} (mg/l). For the conversion to eq/l, the

SO_4^{2-} concentration is divided by 48 mg/eq (molar mass of 96 (g/mol), wherein 1 mol is equal to 2 eq).

After the measurements, the capacity of 25 ml resin can be calculated according to Eq. (2):

$$\text{Capacity} \left(\frac{\text{eq}}{\text{l}} \right) = c(\text{CO}_3^{2-}) \left(\frac{\text{eq}}{\text{l}} \right) + c(\text{Cl}^-) \left(\frac{\text{eq}}{\text{l}} \right) + c(\text{SO}_4^{2-}) \left(\frac{\text{eq}}{\text{l}} \right) \quad (2)$$

In order to normalize the resin capacity, the measured capacity is divided by the resin volume (25 ml).

The maximal NOM removal of a resin can be determined by stirring 50 ml of fresh resin in 1 l of raw influent for 24 h. The evolution of UVA_{254} as a function of time is measured.

The particle size of the resins was examined by laser diffraction on the Mastersizer 2000 (Malvern). With the measured data, equivalent average sizes that take into account the average surface or the average volume of the particles were calculated. Depending on the application, other equivalent diameters can be used. The most common are the Sauter mean diameter ($D[2,3]$) and the De Brouckere mean diameter ($D[3,4]$). The Sauter mean diameter is surface-related and is used in cases where, for example, reactivity and solubility are important. The De Brouckere mean diameter is volume-related and represents the volume that a given number of particles occupy [22].

3. Results and discussion

3.1. Resin properties

The specified average diameters of the two resins used are compared with the measurement results. The resin particle sizes specified by the manufacturer were $740 \pm 110 \mu\text{m}$ (coarse resin) and $570 \pm 50 \mu\text{m}$ (fine resin). The measured particle sizes are quite similar (Table 1). The relative difference in particle size (fine resin compared to the coarser resin) is 18%.

The two resins have, according to manufacturer a density of 1.08 g/ml and an approximate bulk density of 680–730 g/l. The density of both dried (at 100°C for 24 h) and wet resin was measured. The measured density of the dried resin corresponds to the specified density. In this study, the density of the wet resin is important, as this is the density of the resin during the process. The density of the wet resin of the fine resin was $1.04 \pm 0.12 \text{ g/ml}$ while for the coarse resin this was $1.16 \pm 0.06 \text{ g/ml}$.

A distinction is made between the porosity of the resin during operation and the initial porosity (p_0).

Table 1
Properties of the applied resins

Resin	Structure	Water content (%) Measured	Particle size (μm)		Bulk density (g/l)		Density (g/ml)		Capacity (eq/l)		
			Manufacturer's specification	Measured $D[3, 4]$ (μm)	Manufacturer's specification	Measured $D[2, 3]$ (μm)	Manufacturer's specification	Measurement	Manufacturer's specification	Measurement	After regeneration
Fine resin	Macroporous	66–72	585 \pm 116	255 \pm 290	680–730	624 \pm 105	1.08	1.04 \pm 0.12	0.8	0.89	0.63
Coarse resin	Macroporous	66–72	713 \pm 125	316 \pm 354	680–730	572 \pm 119	1.08	1.16 \pm 0.06	0.8	0.88	0.53

First, p_0 is determined theoretically by assuming that the particle size remains the same in wet or dry conditions and it therefore becomes possible to set the porosity of the dry resin equal to the porosity of a (wet) resin. The initial porosity of the resin can be calculated based on Eq. (3), if the bulk density and density are known:

$$p_0 = 1 - \frac{\text{Bulk density } \left(\frac{\text{g}}{\text{l}}\right)}{\text{Density } \left(\frac{\text{g}}{\text{l}}\right)} \quad (3)$$

For both resins with density of 1.08 g/ml and an average bulk density of 705 g/l, this yields an initial porosity of at 0.347 which is lower than the porosity of 0.42 reported for sand filtration [23].

The reported total capacity of both fine and coarse resins is 0.8 eq/l. The measured value for both resins is 0.9 eq/l which corresponds to the specified value (Table 1).

3.2. Evolution of chloride and sulfate ions and conductivity

During the ion exchange process, Cl^- ions are released and not only NOM, but also inorganic ions such as SO_4^{2-} and CO_3^{2-} (present in the water) will be exchanged. The anion resin has a larger affinity for SO_4^{2-} than for NOM.

The removal of DOC and SO_4^{2-} as a function of the number of bed volumes is presented in Fig. 1 for the coarse resin. For the other resin, the results were similar. The EBCT of the test was 60 s. The DOC concentration of the influent averages 10.6 \pm 0.8 mg/l. The SO_4^{2-} concentration of the influent was 71.5 \pm 2.1 mg/l. The conductivity of the influent was 555 \pm 16 mS/cm. The Cl^- concentration was 47 \pm 3 mg/l.

Initially, almost all the SO_4^{2-} ions were removed (94%), while DOC removal was on average 61%. From 600 bed volumes onwards, almost no SO_4^{2-} ions were removed. The DOC removal maintains a fairly constant value at an average of 44%. As such, saturation for DOC removal is not yet reached. The negative removal of SO_4^{2-} after sufficient bed volumes indicates the exchange of SO_4^{2-} for NOM by the resin.

In order to understand Fig. 1, the amount of DOC removed, SO_4^{2-} removed, and Cl^- released are expressed in absolute values (meq/l). For this, all concentrations were recalculated to equivalents per liter. This is straightforward for SO_4^{2-} and Cl^- , while for the number of equivalents per g DOC, the value proposed by Boyer and Singer [24] was used (0.010-eq/g DOC at pH 7). The resulting concentrations are presented in Fig. 2. Initially, (up to 200 bed volumes) more than sufficient Cl^- is released in comparison with the

Table 2

Average influent composition during tests with fine and coarse resin (\pm indicates the standard deviation)

Variable	Average value (tests with fine resin)	Average value (tests with coarse resin)
DOC	9.3 ± 0.9 mg/l	10.6 ± 0.8 mg/l
UVA ₂₅₄	22.6 ± 2.2 l/m	26.1 ± 2.3 l/m
SUVA	2.4 ± 0.3 l/mg m	2.5 ± 0.3 l/mg m
SO ₄ ²⁻	65 ± 14.1 mg/l	71.5 ± 2.1 mg/l
Cl ⁻	50 ± 3 mg/l	47 ± 3 mg/l
Conductivity	552 ± 4 μ S/cm	555 ± 16 μ S/cm

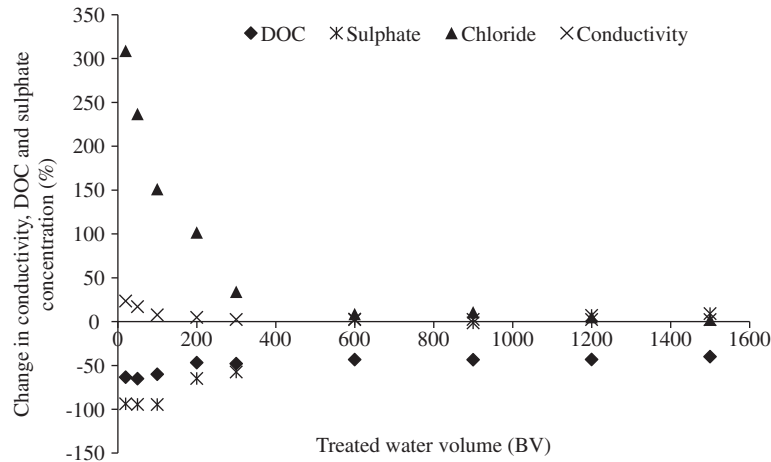
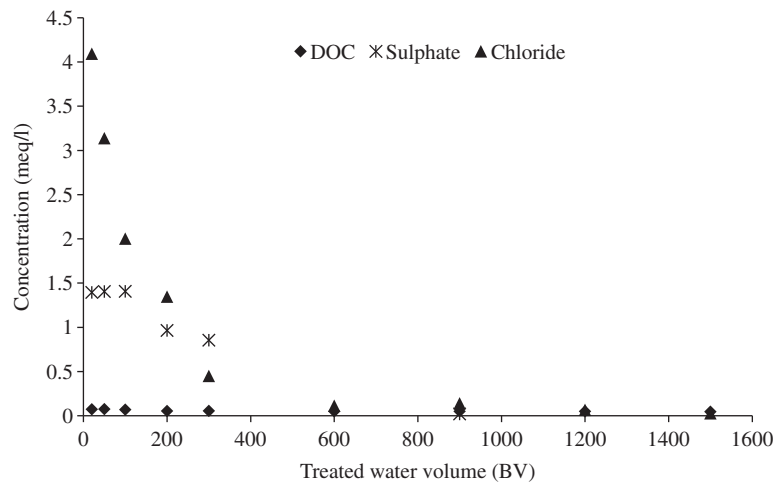


Fig. 1. Relative evolution of DOC, sulphate, chloride and conductivity as function of the number of bed volumes during ion exchange with the coarse resin.

Fig. 2. Removed DOC and SO₄²⁻ and released Cl⁻ expressed as equivalent concentration (meq/l) (data for the coarse resin).

removed DOC and SO₄²⁻. After 20 bed volumes, for example, 4.1-meq/l Cl⁻ is released and 0.07 meq/l DOC and 1.4 meq/l SO₄²⁻ are removed. For higher bed volumes (from 600 bed volumes onwards) on

average 0.08-meq/l Cl⁻ are released, while 0.05 meq/l DOC is removed and on average of 0.07-meq/l SO₄²⁻ is released.

For the other resin similar results were obtained.

3.3. Influence of resin particle size on NOM removal

The influence of the particle size was examined by comparing the behavior of both resins at an EBCT of 60 s. No large difference in terms of DOC removal was noticed between two resins.

At higher bed volumes (300–1,500 BV), where a continuous process is approximated, the DOC removal of the fine resin is on average 8.7% lower than the coarse resin. The results for the same resin exhibit relatively large variations, due to among other things the lower affinity for certain ions (Fig. 3). The initial DOC concentration of the influent for the coarse-resin was on average 10.6 ± 0.8 mg/l, and for the fine resin 9.3 ± 0.9 mg/l.

At low bed volumes, the resins remove on average 83% UV₂₅₄. The UVA₂₅₄ of the influent was 26.1 ± 2.3 1/m for the coarse resin and 22.6 ± 2.2 1/m for the fine resin. The average removal of the fine resin is 5% higher than the coarse resin. From 300 bed volumes onwards, the removals decrease to 57–65% (fine resin) and 62–72% (coarse resin) (Fig. 3). It should be noted that the maximum possible UVA₂₅₄-removal of both resins, measured during a laboratory batch test, is 93%. A complete removal of UVA₂₅₄ is therefore not possible with these resins.

Further, it was checked if a relation exists between UVA₂₅₄ and DOC removal (Δ UVA₂₅₄ (%) and Δ DOC (%)) in the effluent. The data given in Fig. 3 resulted in a linear relation between both measurements. For the coarse resin this relations becomes: Δ DOC = 1.35 Δ UVA₂₅₄ - 39.21 ($R^2 = 0.95$), while for the fine resin this relation becomes: Δ DOC = 1.41 Δ UVA₂₅₄ - 54.94 ($R^2 = 0.88$). Such a relation could enable the online control of DOC removal by the surrogate parameter UV₂₅₄ [20,25,26].

The influent had SUVA values of 2.5 ± 0.3 l/mg m (coarse resin) and 2.4 ± 0.3 l/mg m (fine resin) (Fig. 3). The SUVA removal in this study fluctuates around an average value of $47.1 \pm 11.2\%$ for fine resin and $31.1 \pm 13.1\%$ for coarse resin.

3.4. Influence of regeneration on resin capacity

After several regeneration cycles, it is expected that the resin capacity will decrease because of the irreversible sorption of NOM and wear of the resin. During operation of the column a regeneration with a $\text{Cl}^-/\text{SO}_4^{2-}$ solution (ratio $\text{Cl}^-/\text{SO}_4^{2-} = \pm 3$) was performed after ± 7 runs. The capacity of each resin was measured after the last (7th) regeneration. This value is compared with the fresh resin capacity (Table 1). The concentration of Cl^- in the regeneration solution was 1 eq/l (resulting in a total ionic (Cl^- and SO_4^{2-}) strength of 1.3-eq/l. The capacity of the regenerated coarse resin decreased by 40% (to 0.53-eq/l), while for the fine resin the capacity decreased by 28% (to 0.63 eq/l).

Also the influence of regeneration with a pure SO_4^{2-} was performed. During full-scale application, the regeneration solution is reused and as such an increase in SO_4^{2-} concentration can be expected. Therefore, it is interesting to see the effect of such an increase. Tests were carried out on the column (in which the entire amount of the resin was regenerated) with an EBCT of 60 s. The DOC removal of the resin regenerated with a pure SO_4^{2-} solution is initially similar (after 300 bed volumes) to the DOC removal by the resin regenerated with a the $\text{Cl}^-/\text{SO}_4^{2-}$ solution (data not shown). Also the UVA₂₅₄ removal is similar after 300 bed volumes. From 300 bed volumes

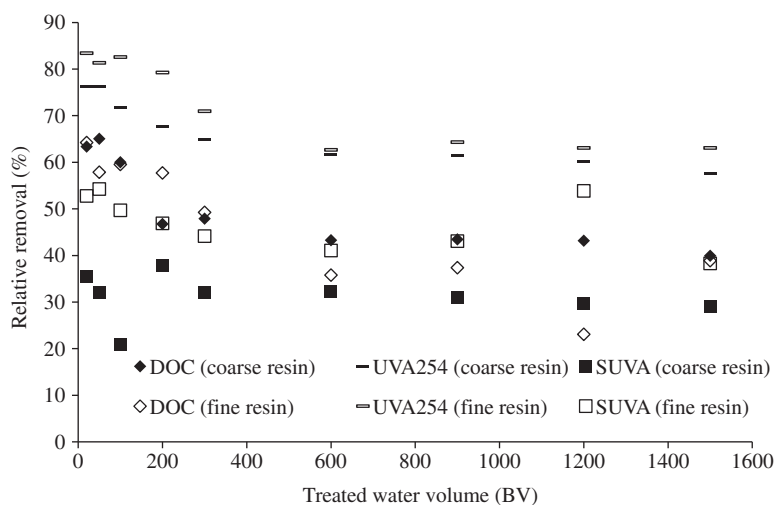


Fig. 3. Performance (expressed as relative removal) comparison between fine and coarse resin.

onwards, the removal of DOC and UVA_{254} remains fairly constant. As such, it can be concluded that in a continuous process, where only 3–4% of the resin is regenerated, that the regeneration ratio will have little impact on the NOM removal efficiency.

3.5. Evolution of spectral properties and molecular size of the NOM

3.5.1. UVA- and DAS spectra

UVA-spectra of the effluent of the column, operated with an EBCT of 60 s were recorded for both resins. Both the fine and the coarse resin showed a similar pattern, with increase in UVA_{254} values when the number of bed volumes increased. In Fig. 4, the results for the fine resin are demonstrated.

NOM gives rise to the formation of DBPs during the oxidation process (e.g. chlorination, ozonation).

The prediction of the potential formation of DBPs can be based on various parameters such as the normalized DAS or DAS at wavelengths around 272 nm. Experiments by Korshin et al. [27,28] in chlorinated water showed that the DAS at this wavelength is strongly related with DBPs [27–29].

The DAS were calculated based on the change in UV-Vis-spectra before and after ion exchange by subtracting the spectra of the effluent from the spectrum of the influent. The NOM components that are not removed are not considered in this spectral profile. The DAS is normalized by dividing the DAS by the DAS-value at the peak wavelength. The peak wavelength was 239 nm (coarse resin) and 240 nm (fine resin). With increasing number of bed volumes, the normalized DAS curves are shifted to the right (Fig. 4, only results from the fine resin are shown).

Prior to 300 BVs, these curves did not coincide which means that the shape of the UV-Vis spectra

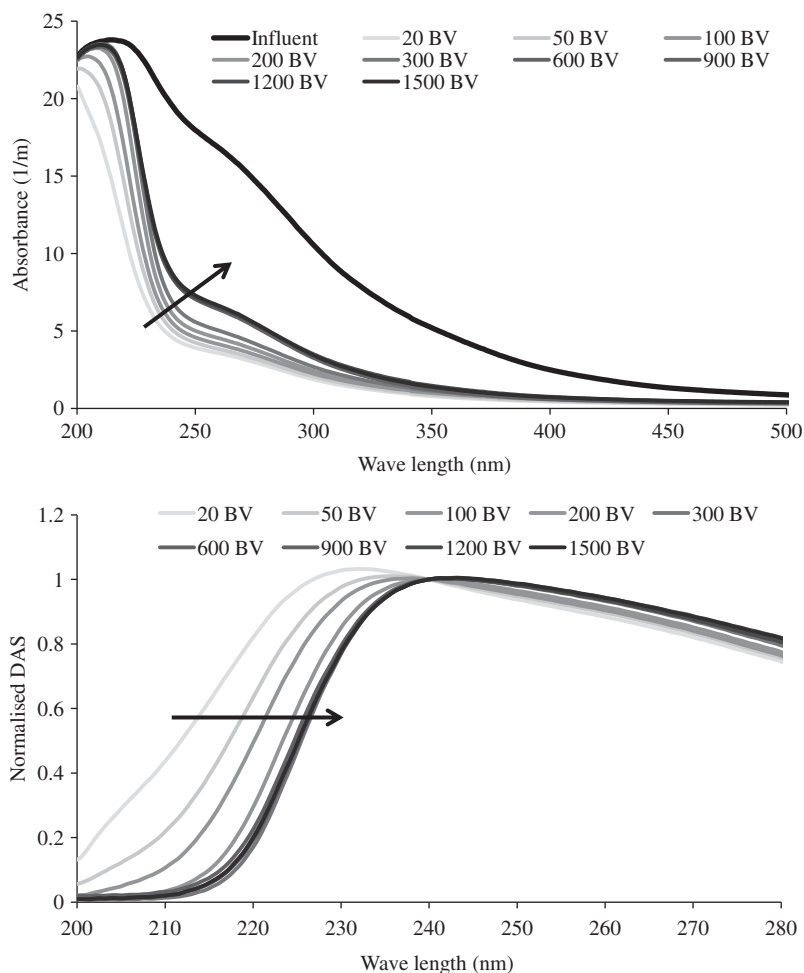


Fig. 4. UVA spectrum of the fine resin of the influent and effluent (as function of the number of bed volumes) (top) and normalized DAS (relative to 240 nm) of the effluent (as function of the number of bed volumes) (bottom).

changed as function of volume treated. Compared to absorption at 240 nm, removal efficiency at lower wavelengths (<240 nm) decreased, while the removal of moieties absorbing at higher wavelengths (>240 nm) slightly increased. This indicates that during the early stage of treatment, interactions between NOM and the resins were different and more NOM moieties could be removed.

3.5.2. Size exclusion chromatography

The HPSEC chromatograms with absorbance at 254 nm give the distribution of apparent MW of NOM in the influent and the treated water (Fig. 5). The influent contains NOM with a MW ranging between 1,400 and 4,000 Da. The largest peak is at $\pm 3,083$ Da, smaller peaks are visible at 1,175 and 2,200 Da. The location and corresponding absorbance of these peaks

or distribution of MW is similar to other surface waters in literature [12–21]. In analogy with the UV–Vis spectra, for both resins a distinction can clearly be made between the measurements up to 300 BVs and the measurements at prolonged treatment. During the initial phase, NOM between 1,500 and 2,500 Da was more removed than at higher BVs.

The decreased removal of lower MW NOM moieties becomes even more clear when the as the relative absorbance decreases. Pore blocking by larger molecules during the course of the treatment might have contributed to this result. Although the coarse resin was expected to have a more open structure, similar results were obtained with both resins.

From the HPSEC results, ASI can be calculated [20,21]. The ASI is, as the DAS, related to the amount of reactive (aromatic) NOM and is as such related with the potential formation of DBPs [20,21]. In Fig. 6,

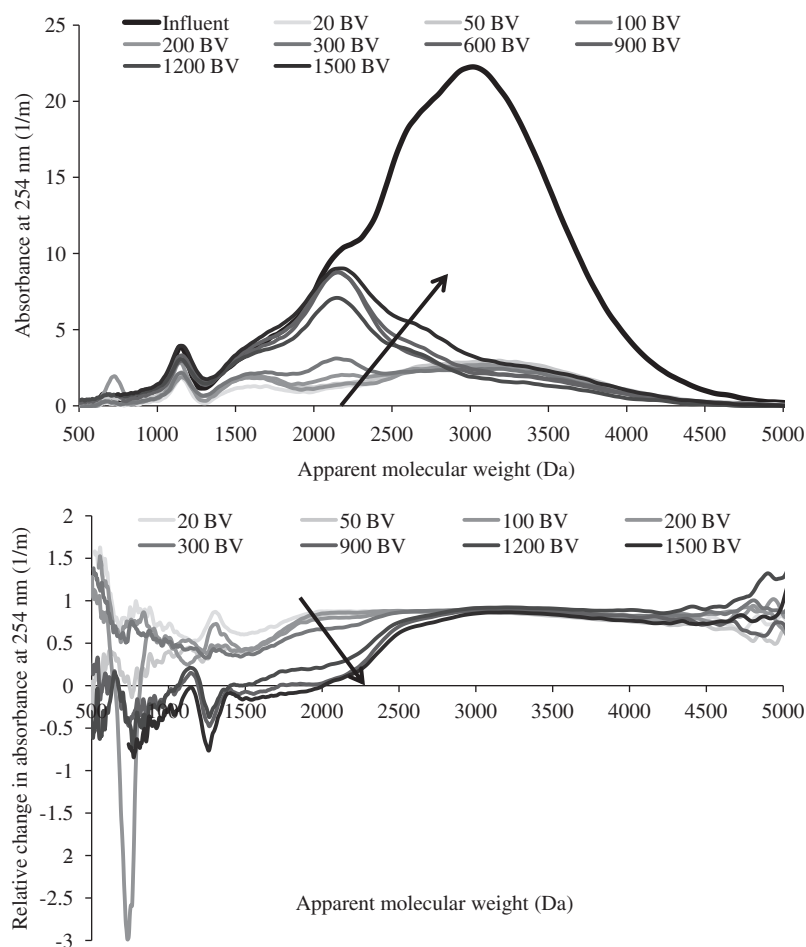


Fig. 5. Measured absorbance at 254 nm of the influent and as function of different bed volumes for experiments with the fine resin as a function of the apparent MW (top) and change in absorbance at 254 nm (relative to the influent) as a function of the apparent MW (bottom).

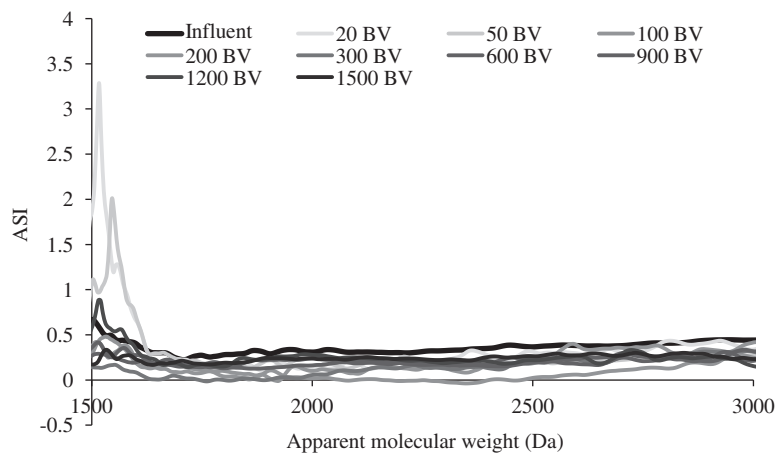


Fig. 6. Calculated ASI of the influent and as function of different bed volumes for experiments with the fine resin as a function of the apparent MW.

the calculated ASI (for measurements with the fine resin) are depicted. In the range between 1,500 and 3,000 Da, a constant ASI with values ranging from 0 to 0.5 was obtained. Outside this region, the ASI varied significantly (data not shown).

3.6. Bed expansion

The bed expansion of the fine and coarse resins was measured and assessed. The theoretical bed expansion increases in proportion to the flow rate of the water (Fig. 7). The measurements of the bed expansion were at 8°C. For flow velocities less than 13 m/h, the measured expansion curves coincide for the fine and coarse resins. Probably, the resins are insufficiently fluidized at these lower flow rates. At

higher flow rates, up to 17.8 m/h, the fine resin expands up to 30% more than the coarse resin.

A theoretical expansion curve can be calculated using the model of Ergun [30]. This model calculates the porosity of a fluidized bed on the basis of the pressure gradient of the bed which is caused by the mass of the resin beads on the one hand and the buoyancy force on the other hand [31]. The comparison makes it possible to calculate the porosity of the resin implicitly (Eq. 4) [31,32].

$$\frac{p^3}{(1-p)^{0.8}} = 130 \frac{v^{1.2} v^{0.8} \rho_w}{g d_p^{1.8} \rho_p - \rho_w} \quad (4)$$

With p is the porosity, v is the viscosity of the water ($1,004 \times 10^{-6} \text{ m}^2/\text{s}$), v is the flow velocity (m/s), ρ_w is the density of the water (1,000 kg/m), g is the acceleration of gravity (9.81 m/s^2), d_p is the particle size of the resin (573 μm), and ρ_p is the density of the resin (1,080 kg/m).

With the calculated porosity (p) of the resin during the ion exchange process, the expansion factor (E) [28] can be calculated by Eq. (5).

$$E = \frac{L}{L_0} = \frac{1-p_0}{1-p} \quad (5)$$

With L is the bed height (m), L_0 is the initial bed height (m), p_0 is the initial porosity, and p is the porosity. The model of Ergun is only valid for Reynolds number between 5 and 100 [31]. This condition is only fulfilled at a flow rate of 0.09 m/h or a flow velocity of 11 m/h (with $Re \approx 5.2$), which is close to the operational conditions of the column.

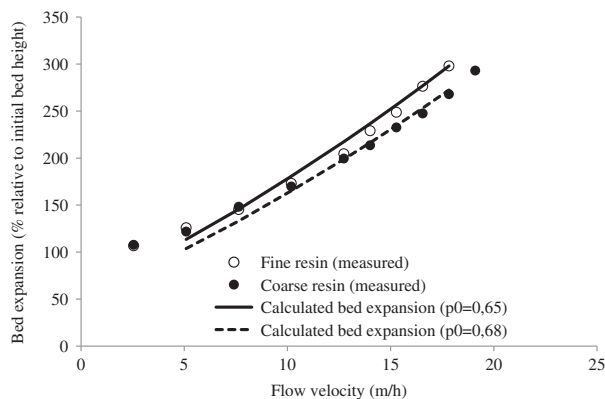


Fig. 7. Bed expansion (measured and theoretical) as function of the flow velocity (relative to the initial height of 25 cm).

For the initially derived initial porosity ($=0.347$, see above), the model of Ergun did not match the experimental data; by fitting the model to the data the initial porosities were estimated. A p_0 of, respectively, 0.65 and 0.68 for the fine and coarse resin is found. The difference with the above derived initial porosity is remarkable and probably the p_0 values are indeed lower, due to the effect of other factors such as the density of the resin which increases during the process.

When extrapolating the model of Ergun to a full-scale application in which a flow velocity of 20 m/h and an initial resin height of 0.5 m would be applied, it becomes clear that the envisioned full-scale plant will have to have a minimum height of 3.5 m.

3.7. Influence of EBCT on NOM removal

The EBCT was varied by allowing the flow rate to vary in the column (up to 160 l/h or 20.4 m/h). Increasing the flow rate leads to a decreased EBCT. Four runs were carried out with the fine resin at 15.3 m/h (performed twice), 11.5, and 7.6 m/h. This corresponds to EBCTs of 60, 80, and 120 s, respectively. The influent UVA₂₅₄ amounted to 22.9 ± 1.9 l/m and the influent concentration of DOC was 9.1 ± 0.6 mg/l. The obtained results show no clear relation between the residence time and the removal of UVA₂₅₄ and DOC. Possibly, there is only a little difference in bed expansion.

Identical tests were conducted with the coarse resin, but that at higher flow rates: 15.3, 17.8, and 20.4 m/h. This results in EBCTs of 60, 51, and 45 s. The influent DOC was 10.8 ± 0.6 mg/l and the influent UVA₂₅₄ was 26.4 ± 1.6 l/m. The removal of UVA₂₅₄ and DOC was quite similar at different flow rates. An increase of the flow rate by 33%, for example, leads to a slight decrease in UVA₂₅₄ removal of on average of 1.2%, while the DOC removal decreased by 0.6%. For a 15% increase in flow rate (17.8–20.4 m/h), this decrease is an average of 0.16% for UVA₂₅₄ and 3.3% for DOC removal.

These obtained results are similar to the earlier tests [19]. The EBCT may thus, as mentioned above, be reduced by increasing the flow rate. The minimum influence of the flow rate on the NOM removal will not always be valid. A maximum or threshold flow rate, at which the removal efficiency decreases significantly, will have to be determined. In addition, the increase of the flow rate will also be limited by the expansion of the resin. Too large expansion leads to an increased pressure drop and a too large resin loss. This latter may be solved by installing a higher column.

4. Conclusion

Two Purolite resins for the removal of NOM from drinking water were compared. NOM removal efficiency was studied as function of EBCT, bed expansion, and regeneration during pilot-scale operation. NOM was characterized based on multiple measurements.

Although the resins differed 18% in size, no significant difference in NOM removal was observed. The exchange capacity of the fine resin (after multiple runs) after regeneration is 12% higher than the coarse resin. The HPSEC results show a similar NOM removal as function of apparent MW. Flow velocity (i.e. EBCT) did not influence the NOM removal significantly within the range of 15–20 m/h. This allows for increasing the flow rate without a major deterioration of the NOM removal, especially since the expansion of the two resins is not a limiting factor.

The $\text{SO}_4^{2-}/\text{Cl}^-$ ratio of the regenerating solution has little influence on the NOM removal efficiency. The accumulation of SO_4^{2-} by the reuse of the regenerating solution does not impede the process.

Although the removal results for both resins were similar, the fine resin was the preferred resin in this case because there are indications for a longer life of the fine resin.

Acknowledgments

The authors would like to thank Jan Cromphout and Liesbeth Verdickt from the Drinking Water Company “De Watergroep” for the collaboration during the experiments and the processing of the data. This project fits within the LED H2O project. The LED H2O belongs to the LED network (www.lednetwerk.be) and is financially supported by The Flanders Knowledge Centre Water (Vlakwa vzw).

References

- [1] G.V. Korshin, Corrosion and Metal Release for Lead-Containing Materials: Influence of NOM, American Water Works Association, Denver, 1999.
- [2] B.H. Kornegay, K.J. Kornegay, E. Torres, Natural Organic Matter in Drinking Water: Recommendations to Water Utilities, American Water Works Association, Denver, 2000.
- [3] A. Matilainen, E.T. Gjessing, T. Lahtinen, L. Hed, A. Bhatnagar, M. Sillanpää, An overview of the methods used in the characterisation of natural organic matter (NOM) in relation to drinking water treatment, *Chemosphere* 83 (2011) 1431–1442.
- [4] T.F. Marhaba, D. Van, The variation of mass and disinfection by-product formation potential of dissolved organic matter fractions along a conventional surface water treatment plant, *J. Hazard. Mater.* 74 (2000) 133–147.

- [5] F. Oesterholt, E. Cornelissen, Karakterisering, Effecten en Verwijdering van NOM Samenvatting NOM- Gerelateerd Onderzoek (Characterization, effects and removal of NOM. Summary of NOM-related research), Watercycle Research Institute, Nieuwegein, 2010.
- [6] D.W. Page, J.A. van Leeuwen, K.M. Spark, M. Drikas, N. Withers, D.E. Mulcahy, Effect of alum treatment on the trihalomethane formation and bacterial regrowth potential of natural and synthetic waters, *Water Res.* 36 (2002) 4884–4892.
- [7] J. Crittenden, R. Trussel, D. Hand, K. Howe, G. Tchobanoglous, *Water Treatment Principles and Design*, second ed., John Wiley & Sons, New Jersey, NJ, 2005.
- [8] C.A. Rokicki, T.H. Boyer, Bicarbonate-form anion exchange: Affinity, regeneration, and stoichiometry, *Water Res.* 45 (2011) 1329–1337.
- [9] W.T.M. Audenaert, M. Callewaert, I. Nopens, J. Cromphout, R. Vanhoucke, A. Dumoulin, P. Dejangs, S.W.H. Van Hulle, Full-scale modelling of an ozone reactor for drinking water treatment, *Chem. Eng. J.* 157 (2010) 551–557.
- [10] T.V. Nguyen, R. Zhang, S. Vigneswaran, H.H. Ngo, J. Kandasamy, P. Mathes, Removal of organic matter from effluents by magnetic ion exchange (MIEX[®]), *Desalination* 276 (2011) 96–102.
- [11] B. Bolto, D. Dixon, R. Eldridge, S. King, K. Linge, Removal of natural organic matter by ion exchange, *Water Res.* 36 (2002) 5057–5065.
- [12] A. Phetrak, J. Lohwacharin, H. Sakai, M. Murakami, K. Oguma, S. Takizawa, Simultaneous removal of dissolved organic matter and bromide from drinking water source by anion exchange resins for controlling disinfection by-products, *J. Environ. Sci. China* 26 (2014) 1294–1300.
- [13] M.R.D. Mergen, B. Jefferson, S.A. Parsons, P. Jarvis, Magnetic ion-exchange resin treatment: Impact of water type and resin use, *Water Res.* 42 (2008) 1977–1988.
- [14] H. Humbert, H. Gallard, H. Suty, J.P. Croué, Performance of selected anion exchange resins for the treatment of a high DOC content surface water, *Water Res.* 39 (2005) 1699–1708.
- [15] E.R. Cornelissen, N. Moreau, W.G. Siegers, A.J. Abrahamse, L.C. Rietveld, A. Grefte, M. Dignum, G. Amy, L.P. Wessels, Selection of anionic exchange resins for removal of natural organic matter (NOM) fractions, *Water Res.* 42 (2008) 413–423.
- [16] M. Slunjski, K. Cadee, J. Tattersall, MIEX[®] resin water treatment process, in: *Proceedings of Aquatech Amsterdam*, The Netherlands, 2000, pp. 26–29.
- [17] D. Hongve, J. Baann, G. Becher, O.A. Beckmann, Experiences from operation and regeneration of an anionic exchanger for natural organic matter (NOM) removal, *Water Sci. Technol.* 40 (1999) 215–221.
- [18] E.R. Cornelissen, E.F. Beerendonk, M.N. Nederlof, J.P. van der Hoek, L.P. Wessels, Fluidized ion exchange (FIX) to control NOM fouling in ultrafiltration, *Desalination* 236 (2009) 334–341.
- [19] L. Verdickt, W. Closset, V. D’Haeseleer, J. Cromphout, Applicability of ion exchange for NOM removal from a sulfate-rich surface water incorporating full reuse of the brine, *Water Sci. Technol.: Water Supply* 12 (2012) 878–887.
- [20] W.T. Audenaert, D. Vandierendonck, S.W. Van Hulle, I. Nopens, Comparison of ozone and HO₂. Induced conversion of effluent organic matter (EfOM) using ozonation and UV/H₂O₂ treatment, *Water Res.* 47 (2013) 2387–2398.
- [21] G. Korshin, C.W.X. Chow, R. Fabris, M. Drikas, Absorbance spectroscopy-based examination of effects of coagulation on the reactivity of fractions of natural organic matter with varying apparent molecular weights, *Water Res.* 43 (2009) 1541–1548.
- [22] T. Allen, *Particle Size Measurement*, fourth ed., Chapman and Hall, New York, NY, 1990.
- [23] A.P. Arcadio, G.A. Sincero, *Physical-Chemical Treatment of Water and Wastewater*, IWA Publishing, London, UK, 2002.
- [24] T.H. Boyer, P.C. Singer, A pilot-scale evaluation of magnetic ion exchange treatment for removal of natural organic material and inorganic anions, *Water Res.* 40 (2006) 2865–2876.
- [25] T. Anumol, M. Sgroi, M. Park, P. Roccaro, S.A. Snyder, Predicting trace organic compound breakthrough in granular activated carbon using fluorescence and UV absorbance as surrogates, *Water Res.* 76 (2015) 76–87.
- [26] M. Chys, V.A. Oloibiri, W.T.M. Audenaert, K. Demeestere, S.W.H. Van Hulle, Ozonation of biologically treated landfill leachate: Efficiency and insights in organic conversions, *Chem. Eng. J.* 277 (2015) 104–111.
- [27] G.V. Korshin, W.W. Wu, M.M. Benjamin, O. Hemingway, Correlations between differential absorbance and the formation of individual DBPs, *Water Res.* 36 (2002) 3273–3282.
- [28] G.V. Korshin, C.W. Li, M.M. Benjamin, The decrease of UV absorbance as an indicator of TOX formation, *Water Res.* 31 (1997) 946–949.
- [29] P. Roccaro, H.S. Chang, F.G.A. Vagliasindi, G.V. Korshin, Differential absorbance study of effects of temperature on chlorine consumption and formation of disinfection by-products in chlorinated water, *Water Res.* 42 (2008) 1879–1888.
- [30] S. Ergun, Fluid flow through packed columns, *Chem. Eng. Prog.* 48 (1952) 89–94.
- [31] K.M. van Schagen, L.C. Rietveld, R. Babuška, O.J.I. Kramer, Model-based operational constraints for fluidised bed crystallisation, *Water Res.* 42 (2008) 327–337.
- [32] J. Van Dijk, D. Wilms, Water treatment without waste material—Fundamentals and state of the art of pellet softening, *J. Water Supply Res. Technol.-Aqua* 40 (1991) 263–280.